

Article

Fatigue Loads Estimation Through a Simple Stochastic Model

Pedro G. Lind, Iván Herráez, M. Wächter, J. Peinke

ForWind - Center for Wind Energy Research, Institute of Physics,
Carl von Ossietzky University of Oldenburg, 26111 Oldenburg, Germany

* Author to whom correspondence should be addressed; Email: pedro.g.lind@forwind.de, Phone:
+49(0)4417985051, Fax: +49(0)4417985099

Received: xx / Accepted: xx / Published: xx

Abstract: We propose a procedure to estimate the fatigue loads on wind turbines, based in a recent framework used for reconstructing data series of stochastic properties measured at wind turbines. Through a standard fatigue analysis, we show that it is possible to accurately estimate fatigue loads in any wind turbine within one wind park, using only the load measurements at one single turbine and the set of wind speed measurements. Our framework consists of deriving a stochastic differential equation that describes the evolution of the torque at one wind turbine driven by the wind speed. The stochastic equation is derived directly from the measurements and is afterwards used for predicting the fatigue loads at neighboring turbines. Such a framework could be used to mitigate the financial efforts usually necessary for placing measurement devices in all wind turbines within one wind farm. Finally, we also discuss the limitations and possible improvements of the proposed procedure.

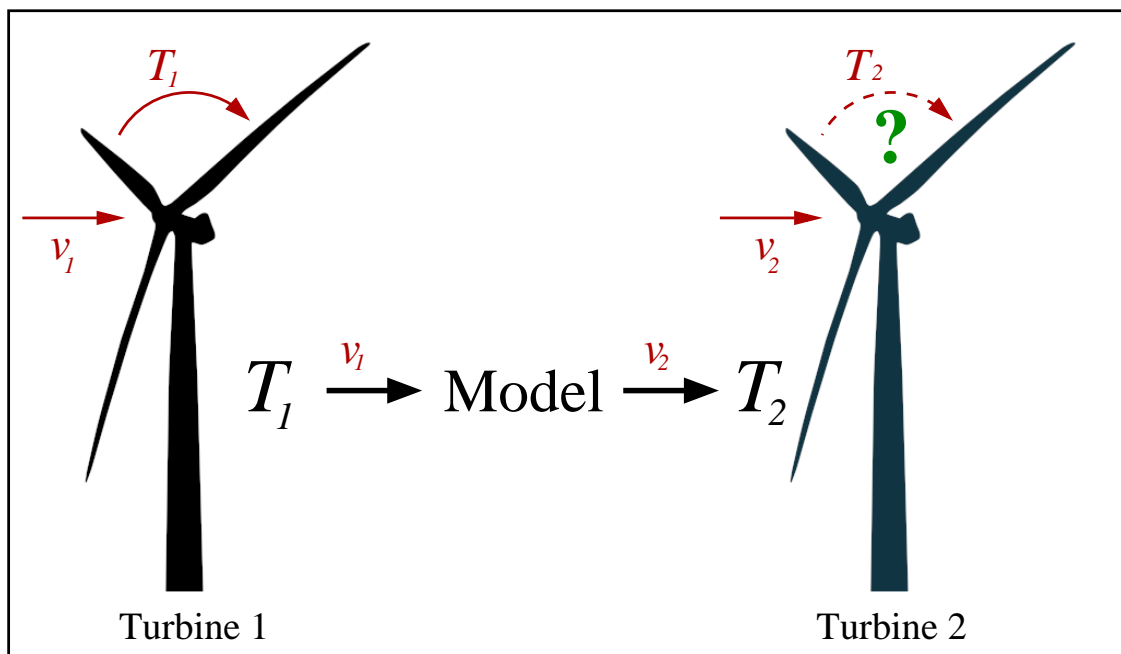
Keywords: Fatigue loads; Stochastic Modeling; Langevin Equation

1. From the load at one single turbine to the fatigue of an entire wind farm

Wind energy has become one of the most promising answers to the world-wide energetic problem[1], profiting from the recent developments and research activities in engineering, meteorology and physical sciences. However, important challenges still remain to be solved, particularly in two fronts.

First, in what concerns the predictability and optimization of power production when the wind is itself turbulent and intermittent[2], i.e. large fluctuations occur with a non-negligible probability[3].

Figure 1. Sketch of the proposed idea for estimating fatigue loads: one derives a stochastic model from the data series of the wind speed and torque measured at Turbine 1; using this model and the wind speed series measured at the Turbine 2 one reconstructs the statistics of the torque at the Turbine 2; from the estimated torque series one estimates fatigue loads. This procedure can theoretically be applied to other properties one wants to access for monitoring and controlling wind turbines, avoiding to place measurement devices in all of them (see text).



Second, the costs implied in the construction of wind turbines together with the proper devices for controlling and monitoring them are typically high[4]. Alternative methods to indirectly estimate the necessary quantities for control and monitoring could help to mitigate these costs.

Both these two different types of challenges in wind energy research are in fact related with each other. An important example is that devices for measuring certain types of loads are considerably expensive, and due to the unpredictable and intermittent nature of the wind, one typically places one or more devices at each turbine, for preventing loss of accuracy in cumulative loads[5,6]. The loads applied on one wind turbine are important to estimate, within some accuracy, the life expectancy of a turbine or the maximal time-span between two inspections of its operating features. Moreover, knowing how the applied loads evolve in time helps understanding the fatigue behavior and critical situations that compromise the functionality of the turbine[7]. Therefore, establishing models for the intermittency of the loads in single wind turbines would not only contribute for better understanding the energy production and the monitoring of wind turbines, but would also open the possibility for mitigating expensive procedures.

In this paper we propose a recent model for reconstructing the increment statistics of the torque in single wind turbines as a tool for estimating fatigue loads, not only of that wind turbine but also of their neighboring ones. As sketched in Fig. 1 we use the wind speed and torque data series of one wind turbine (Turbine 1) to derive our stochastic model that describes statistically the evolution of the torque subject to the observed wind speed. We assume that the response of similar wind turbines to the wind speed

shall yield similar values of their properties, such as the power, the blade bending moments or the torque on the main shaft. Therefore, we apply the derived stochastic model to another wind turbine (Turbine 2) where only the wind speed is measured on the nacelle. The outcome yields a series of torque estimates used for a fatigue analysis, including Markov matrices, rainflow counting statistics and load duration distribution, which are then compared with the fatigue analysis of the respective torque measurements. The overall result is that our stochastic model retrieves accurate estimates of fatigue loads in any wind turbine within the same wind farm.

We start in Sec. 2.1 by describing the data analyzed and in Sec. 2.2 the method is described in further detail. Our results for extracting the stochastic model are described in Sec. 3.1 and the fatigue analysis and fatigue estimate are presented and discussed in Sec. 3.2. Section 4 concludes the paper.

2. Data and methodology

2.1. Wind speed and torque in Alpha Ventus

We analyze the set of measurements of the wind speed and torque taken at two different wind turbines of Senvion in Alpha Ventus wind farm, namely turbines AV4 and AV5, during the full month of January 2013.

In principle, our analysis could also be done for other types of loads instead of the drive torque. However, in this article we focus on the fatigue on the drive train, since some of its components are known to be prone to failure. In the future, we aim at extending our analysis to other turbine components.

Figure 2 shows a sketch of the Alpha Ventus wind farm, the first off-shore wind farm in Germany, located at Borkum West in the North Sea, 54.3°N-6.5°W. As shown in the wind rose, during January 2013 the main wind direction lies between Northeast and East.

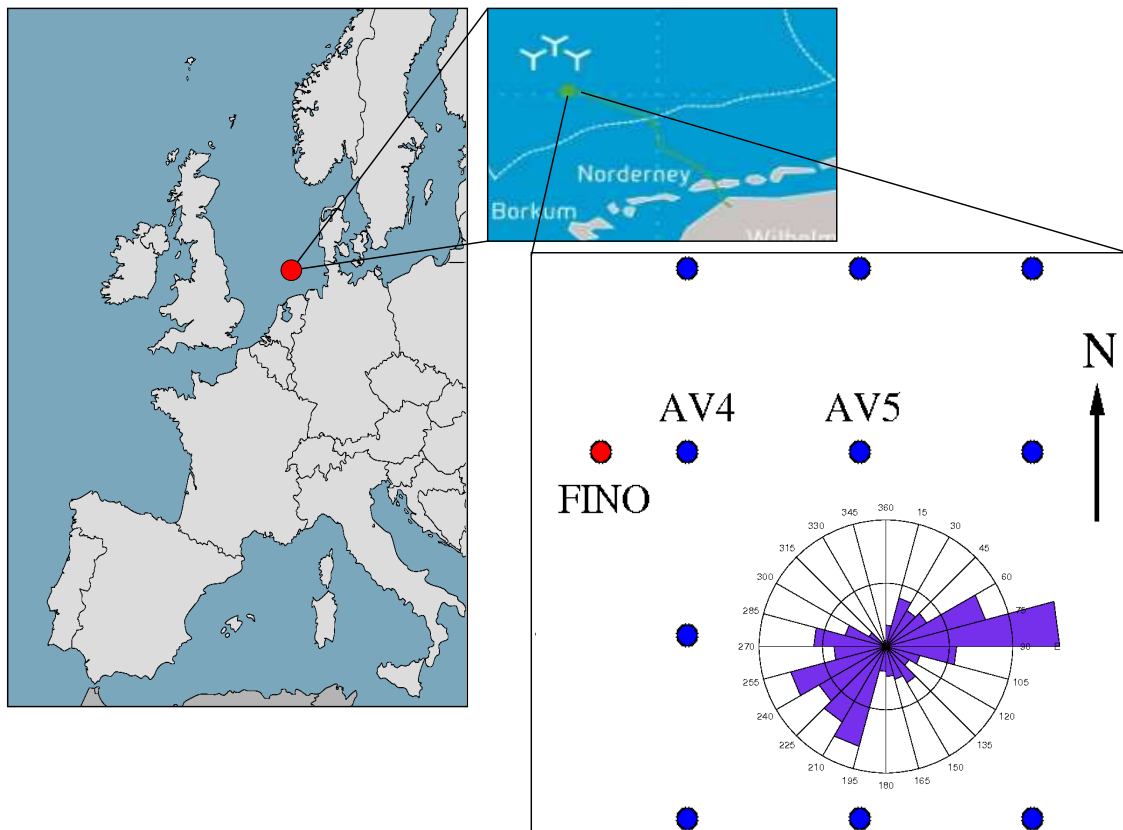
The torque on the main shaft T is computed from the measurements of the power output P and the rotor rotational speed n , assuming neither mechanical nor electrical losses,

$$T = \frac{30 P}{\pi n} \quad (1)$$

with n in r.p.m., P in W and T in Nm. The sampling rate of the power output, rotational speed and consequently the torque is 50 Hz and the sampling rate of the wind speed is 1 Hz. Since we need to use the same sampling rate for all data series, we only consider torque measurements each second, at instants for which a wind speed measurement also exists. In total, for turbine AV4, we have 826745 data points.

Both the wind speed and torque measurements are shown in Fig. 3 and are according to the torque-speed curve known in the literature[4,8,9]. As one sees, the torque at both wind turbines, in Figs. 3a and 3c, shows periods of high power production (large values), alternating with pronounced decreases and subsequent increase during which large fluctuations occur. The largest values of the torque observed for turbine AV4 (Fig. 3a) are not so close to the maximum observed value as the values observed in the torque at AV5 (Fig. 3c). As for the wind speed observed in both turbines (Figs. 3b and 3d) it increases and decreases in an oscillating manner and simultaneously in both turbines, but showing no clear periodic pattern. In Fig. 3e one also plots the joint probability density function (PDF) for both

Figure 2. Sketch of the Alpha Ventus wind farm, located in the North Sea, near the northeastern coast of Germany. The study here described is based on measurements taken at the two wind turbines AV4 and AV5, manufactured by Senvion SE. In the period of January 2013, during which the measurements analyzed in this paper were taken, the wind direction show a tendency towards East-northeast.



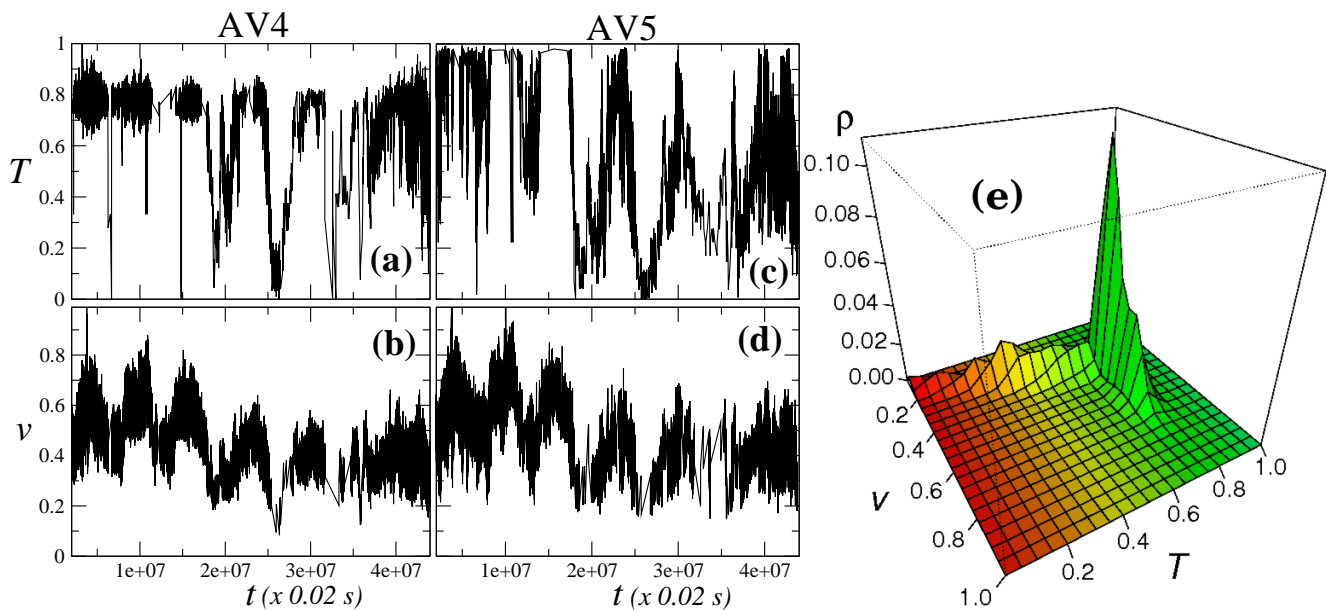
the wind velocity and the torque, a plot that will be of importance when interpreting the stochastic model introduced below.

All data series were analyzed according to all confidential protocols and were properly masked through the normalization by their highest value, being here published with Senvion's permission. Scientific conclusions are not affected by such data protection requirements.

Together with most of the properties measured at wind turbines, wind speed and torque have typically fluctuations occurring at different time-spans, defining series of increments, whose statistics describe the intermittency observed in the wind energy production[10]. In the particular case of the torque, the succession of torque increments are related with the so-called random load cycles which are of importance for estimating fatigue loads.

From the physical point of view the fatigue load at one wind turbine is roughly the time integral of load increments, or of some proper positive and monotonic function of the increments. Therefore, we consider the increments $\Delta T_{\tau}(t) = T(t + \tau) - T(t)$, taken with a fixed time-gap τ . As reported in Ref. [9], for up to one hour or more, the torque increment distributions are clearly non-Gaussian. In Sec. 2.2 we will describe a framework which yields an evolution equation for the torque constrained to the wind speed observed at the same turbine. With such a framework we reconstruct not only the torque

Figure 3. The torque and wind speed measured at turbines AV4 and AV5 from Senvion in Alpha Ventus wind farm. All data was masked through normalization to the largest values (see text). For constructing the stochastic model, one uses (a) the torque T and (b) the wind speed v at AV4, for estimating (c) the torque at AV5 conditioned to its (d) wind speed. In (e) we show the histogram on the observed pair of torque and wind velocity measurements taken at turbine AV4. In both T and v 21 bins were used to cover the full range of values $[0, 1]$. This histogram will be of importance when addressing Fig. 5.



observed at that same wind turbine, but also the torque observed in neighboring wind turbines which we assume to respond similarly to the wind speed.

2.2. The conditional Langevin model for turbine loads

The Langevin approach is a framework developed from the pioneer work by Peinke and Friedrich in 1997[11], which consists of a direct method for extracting the evolution equation of stochastic series of measurements. Several applications were proposed and developed, e.g. in turbulence modeling, in medical EEG monitoring and in stock markets. See Ref. [12] for a review. In the context of wind energy, this framework has shown the ability for predicting power curves of single wind turbines[10,13,14] as well as of equivalent power curves for entire wind farms[15], and also to properly reproduce the increment statistics of power and torque in single wind turbines[9,10].

One considers a set of measurements $X(t)$ in time t of one particular property x evolving according to the so-called Langevin equation defined by

$$\frac{dx}{dt} = D^{(1)}(x) + \sqrt{D^{(2)}(x)}\Gamma_t, \quad (2)$$

where Γ_t is a Gaussian δ -correlated white noise, i.e. $\langle \Gamma(t) \rangle = 0$ and $\langle \Gamma(t)\Gamma(t') \rangle = 2\delta_{ij}\delta(t - t')$.

The first term in the right hand-side incorporates the deterministic contributions in the process, yielding the drift function $D^{(1)}$, while the second terms models the diffusion, i.e. the total stochastic contributions accounting for the stochastic fluctuations, which are incorporated by function $D^{(2)}$. The

constant in δ -correlation and the square root in the Langevin equation are usually chosen for convenience. Details can be found in Ref. [12].

Since the drift and diffusion function have a physical interpretation, one could apply the model in Eq. (2) to a particular system and define *ad hoc* the functional shape of both functions from physical reasoning. In several cases however such approach is not convenient. For instance, when considering properties which result from the interaction between a turbulent system, such as the atmosphere, and a complex technical device, such as the drive train in a wind turbine. In those cases, it is hard to derive drift and diffusion from first principles and the one natural alternative to get information about their functional form is data analysis. In this work we deal, therefore, with the inverse problem: having a set of measurements is it possible to derive the drift and diffusion functions in order to reproduce the statistics of that set of measurements from simple integration of Eq. (2)?

The short answer is yes, it is possible. The long answer has two main steps.

In the first step, one needs to test the data to ascertain if it can be taken as a Markovian series, i.e. if there is a time interval t_ℓ , so-called the Markov-Einstein length, for which in the succession of measurements the next value only depends on the present one and is independent of the values previous to it. In other words, one must test if

$$\rho(X(t+t_\ell)|X(t), X(t-t_\ell), X(t-2t_\ell), \dots) = \rho(X(t+t_\ell)|X(t)) \quad (3)$$

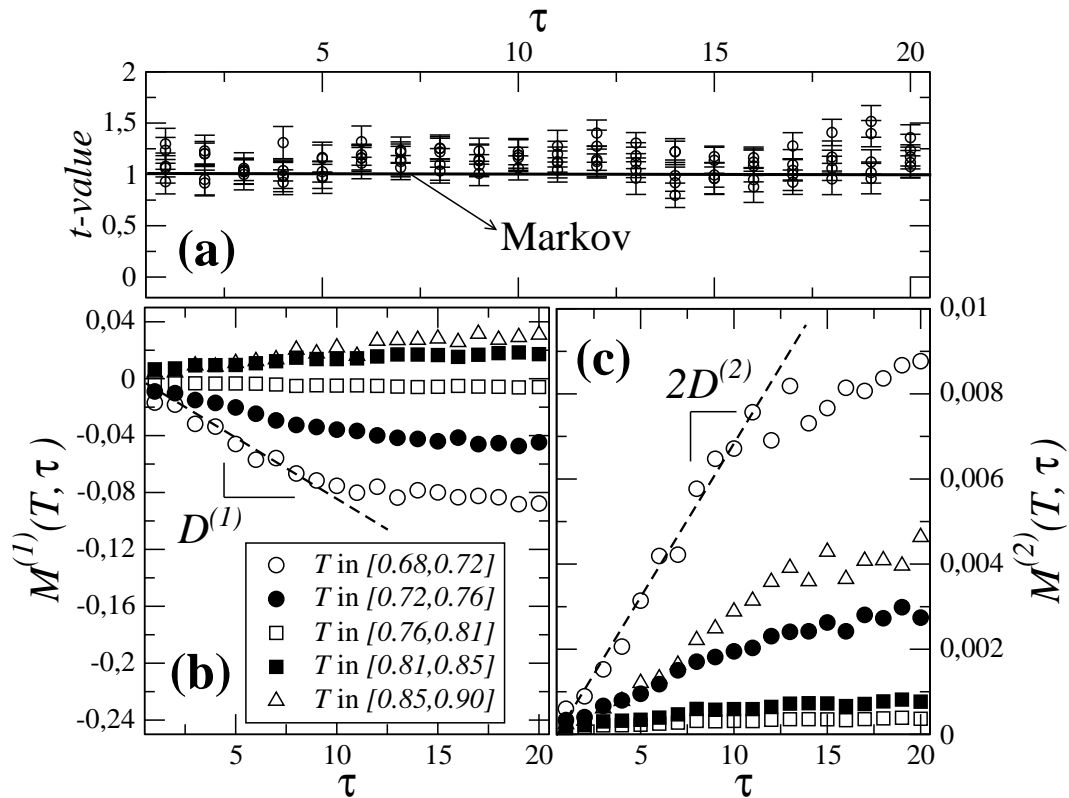
holds, with $\rho(x|y)$ representing the conditional probability density function (PDF) for observing x having observed y . This PDF can be extracted from histograms of the data set.

There are simple standard ways to perform this test[12], which typically compare three-point statistics such as $\rho(X(t+t_\ell)|X(t), X(t-t_\ell))$ conditioned to a fixed value $X(t-t_\ell) = X^*$, with the corresponding two-point statistics $\rho(X(t+t_\ell)|X(t))$ and ascertain for which t_ℓ one obtains the best overlap, between both PDFs.

Though, when the measurements obey this Markov condition the next step can be carried out, one advantage of this Langevin framework is that it also works in some cases where the Markov test fails. One of such cases is the presence of measurement noise[16,17], which opens a broad panoply of different practical situations where this framework is applicable. In the present case, though no measurement noise seems to be present, as reported below, the Markov condition is not perfectly fulfilled as shown in Fig. 4a. Still, important to stress here, it is possible to accurately estimate fatigue loads using such a framework.

To test the Markov condition we compute a t -value as shown in Fig. 4a. The Wilcoxon test is a statistical test used to test if Eq. (3) holds. One assumes to have two different series of values from independent random variables and tests whether the variables are identically distributed or not. The model retrieves a t -value, which when equal to unit indicates perfect matching between both distributions in Eq. (3). As we see from Fig. 4a, though the observed t -values lie near the perfect fit value, they can not always be taken as being one within numerical precision. Still, as we explain below, such fact does not prevent us for accurately estimate fatigue loads.

Figure 4. The Markov-Wilcoxon test retrieves a normalized t -value which taking the value 1 (solid line) indicates perfect matching between the two condition probability distributions. **(a)** In the load series conditioned to wind velocity values the Markov condition is not perfectly fulfilled, but the method is still able to reproduce accurate estimates (see text). For that estimate one starts by computing **(b)** the first and **(c)** the second conditional moments as defined in Eqs. (4). As indicated with dashed lines the slope observed yields the values for the drift and diffusion equation (see Eq. (5)).



For the second step, one needs to derive both functions, $D^{(1)}$ and $D^{(2)}$, that fully define Eq. (2). The derivation is performed through the computation of the corresponding first and second conditional moments[9], respectively

$$M^{(1)}(x, \tau) = \langle X(t + \tau) - X(t) \rangle |_{X(t)=x} \tag{4a}$$

$$M^{(2)}(x, \tau) = \langle (X(t + \tau) - X(t))^2 \rangle |_{X(t)=x} \tag{4b}$$

where $\langle \cdot \rangle |_{X(t)=x}$ indicates the average over the full time series, whenever $X(t)$ takes the value x .

Figures 4b and 4c show the first and second conditional moments for five different values of the torque at AV4. By taking the slope of the linear regression for each conditional moment yields the corresponding coefficient $D^{(1)}$ and $D^{(2)}$. Indeed, it can be shown[18] that drift and diffusion functions in Eq. (2) are, apart from a multiplicative constant ($1/k!$), the derivative with respect to the time-gap τ of the first and second conditional moments respectively, which for arbitrary order k is defined as

$$D^{(k)}(x) = \lim_{\tau \rightarrow 0} \frac{1}{k!} \frac{M^{(k)}(x, \tau)}{\tau} \tag{5}$$

Therefore, drift ($k = 1$) and diffusion ($k = 2$) can be directly extracted from the data sets. For accuracy purposes a correction is introduced for the diffusion function[19], where instead of the second condition moment $M^{(2)}(x, \tau)$ one considers

$$M_{cor}^{(2)}(x, \tau) = M^{(2)}(x, \tau) - [M^{(1)}(x, \tau)]^2. \quad (6)$$

Within a sufficiently low range of τ values, typically between five and ten time-steps of the set of measurements, the conditional moments depend linearly on τ . Thus, for each value x , both $D^{(1)}(x)$ and $D^{(2)}(x)$ are given by the slope of the linear interpolation of the corresponding conditional moments.

It is worth mentioning that, as known in previous studies[16,17], the existence of an offset in the conditional moments indicates the presence of measurement noise in the data. As shown in Figs. 4b and 4c the linear interpolations cross the origin and no offset seems to exist. Therefore one can say that measurement noise is not significant in data sets analyzed in this paper.

On top of these two steps, one important assumption must be added: the set of measurements must be stationary. This is of course *not* the case for torque series at one wind turbine. To overcome this shortcoming, it was recently proposed that[9,20] one should consider the succession of measurements of the torque corresponding to a sufficiently narrow range of speed values. Considering only this subset of torque values governed by what we named the conditioned Langevin equation[9], one observes that the statistical moments of the torque values distribution are approximately constant, depending only on the wind speed (not shown). The conditioned Langevin equation used here as model is defined as

$$\frac{dT}{dt} = D^{(1)}(T, v) + \sqrt{D^{(2)}(T, v)}\Gamma_t, \quad (7)$$

where, for our purposes, T represents the torque at the wind turbine and v is the wind speed.

For such extension of the Langevin approach, now conditioned to the values the wind velocity, all the procedure described above is applied separately for value of the wind velocity. This means that, having the full series of the torque at AV4, one now filters out all values except those observed together with a given wind velocity $v = v^*$ and computes, one for them, the conditional moments:

$$M^{(1)}(T, \tau) = \langle T(t + \tau) - T(t) \rangle |_{T(t)=T, v(t)=v^*}, \quad (8a)$$

$$M^{(2)}(T, \tau) = \langle (T(t + \tau) - T(t))^2 \rangle |_{T(t)=T, v(t)=v^*}. \quad (8b)$$

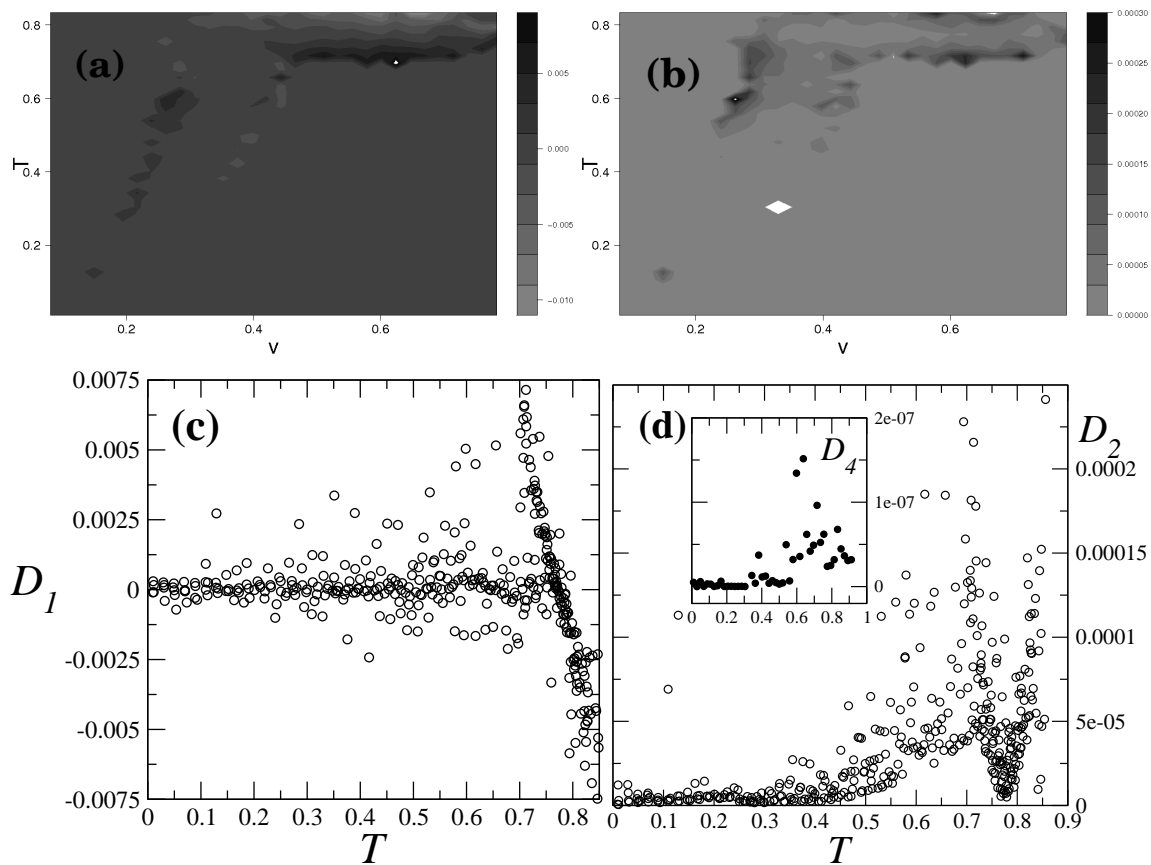
Similarly, the Markov test was also performed for each wind velocity separately, as described above.

Having derived both drift and diffusion functions a final test must be performed. Generically, one can compute from Eqs. (5) the coefficients $D^{(k)}(x)$ of an arbitrary order k . However, according to Pawula's theorem[18], in the case that $D^{(4)}$ is zero or, for practical purposes, it is negligible in comparison with the drift and the diffusion, all coefficients of order $k \geq 3$ are also negligible.

Figure 5a and 5b show the drift and diffusion respectively as a function of both the torque and the wind velocity. The projection along the velocity is shown in Figs. 5c and 5d where one identifies a transition approximately at $T = 0.75$ where the drift depends linearly on the torque, while the diffusion depends quadratically on the torque.

From the plots 5a and 5b one sees that the value $T = 0.75$ is first attained for wind velocities around $v = 0.4$. These two values also separate two different regions when observing the joint PDF (see Fig. 3e).

Figure 5. Numerical result for (a) the drift $D^{(1)}(T, v)$ and (b) the diffusion $D^{(2)}(T, v)$ in the Langevin equation (7) from which the time series of the torque is reconstructed. In (c) and (d) one plots the corresponding integration over the wind speed. The numerical values of both functions are the ones used for predicting the torque series in wind turbine AV5. In the inset one sees the lower values of $D^{(4)}$ which enables us to only consider drift and diffusion (see text). Here, only the range $[0, 0.85]$ is plotted; as shown in Fig. 3e beyond this range no significant statistics is observed. Both $D^{(1)}$ and $D^{(2)}$ were computed for 21 bins in the torque, covering only the observed range of values at each particular velocity bin (21 bins).



Above this value the controller at a wind turbine starts operating. Below that velocity the drift is almost absent and diffusion decays with the magnitude of the velocity. Considering Eq. 7, a closer look into the plots in Fig. 5 enables one to physically interpret $D^{(1)}$ and $D^{(2)}$ in a stochastic model for the torque conditioned to the wind velocity.

In general [18], the drift measures the force driving a specific property to increase or decrease in time, while the amplitude in the diffusion coefficient measures the amplitude of a fluctuation around that driven motion. Having such physical interpretation in mind and looking again to the plots in Fig. 5 one can conclude that the controller starts operating around $v = 0.4$. Indeed, for this value the drift coefficient $D^{(1)}$ shows a linear dependence on the torque with a negative slope: when the torque increases the controller acts in order to decrease it and vice-versa. Simultaneously, diffusion depends quadratically on T . Moreover, below the velocity threshold for controller operation the drift almost vanishes with a diffusion that decreases with the magnitude of the wind velocity: no force is driving the torque for this range of wind velocities and the magnitude of torque fluctuations increases with the wind velocity.

3. The stochastic model for fatigue loads

Using the Langevin framework described in the previous section, we next apply it to wind turbine AV4 in order to extract a stochastic model for the torque, that is assumed to hold for any Alpha Ventus turbine of the same model. Then, we use the set of wind speed measurements at a different wind turbine, namely AV5, for generating the increments of the torque at this second turbine and compare it with the torque measurements. Finally we show that the estimate of the fatigue loads at wind turbine AV5 are statistically the same for the empirical torque measurements and for the reconstructed series.

3.1. Reconstruction of non-stationary time-series

In a previous paper[9] we have shown that the anomalous wind statistics are responsible for the intermittent time evolution of the load in single wind turbines, promoting additional fatigue of the turbine itself. The approach used there follows from the method proposed in Ref. [3,10] to the power output of single turbines.

We now use the model introduced in our previous work, with the drift and diffusion functions, $D^{(1)}$ and $D^{(2)}$ in Fig. 5, extracted according to the framework described above for turbine AV4, and apply it to generate the torque in a neighboring wind turbine, namely AV5.

The wind speed measurements taken at AV5 are used as input data, and initialize the differential evolution equation, Eq. (7), with the first measurement of the torque at this same wind turbine. The reconstruction of the increment statistics is plotted in Fig. 6 with solid lines together with the empirical distributions in dashed lines. While for low values of the time-span τ the extreme fluctuations are not completely well reproduced, above a time window larger than a few seconds the fit between measurements and model is very good.

In the inset of Fig. 5b one sees that the typical values of $D^{(4)}$ are of the order of 1 to 2 % of $D^{(2)}$ values. As explained above, such low values corroborate the applicability of the method to these data sets.

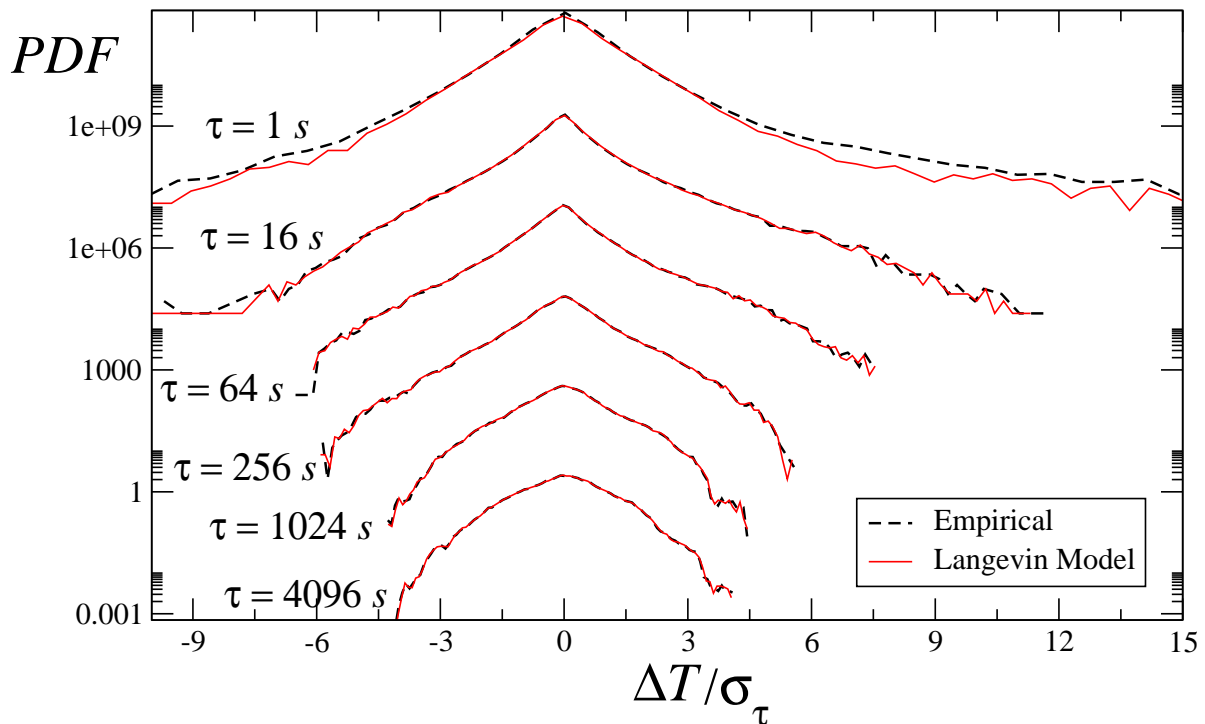
For practical purposes, one should briefly stress that the model here described is suitable for cases where the sampling frequency of the wind speed and torque data is high enough. A sparse sampling of the wind speeds leads to a poor increment statistic and consequently is not accurate enough for estimating fatigue loads.

Having a proper way for reconstructing the increment statistics, one is now in position to use the reconstructed series of loads for estimating the fatigue at AV5 and compare it with the empirical fatigue analysis.

3.2. Fatigue analysis and estimate

To test the capability for the Langevin framework to predict fatigue loads in a wind farm, we next present a comparative fatigue analysis between both the empirical data sets at AV4 and AV5 and the reconstructed data set for AV5 only. This comparative analysis is based on three standard tools, namely Markov matrices of the number of cycles, the rainflow counting procedure and the load duration

Figure 6. Reconstruction of the probability density function of the increments (fluctuations) of the torque at turbine AV5. Time is in seconds, and the torque increments is in units of corresponding standard deviations (σ_τ).



distribution. All these tools are based in the concept of load cycle which is the observed load fluctuation between two successive local minima or maxima of the load.

The rainflow-counting method was proposed in the late sixties by Endo and Matsuishi[21] and became the most standard algorithm for cycle-counting during the last decades, due to its ability for accurately predicting the fatigue loads in a sequence of non-constant cycles. In short, this method aims to count the number of local maxima and minima weighting each one by its increment fluctuation, defined mathematically by Rychlik in Ref. [22] as follows.

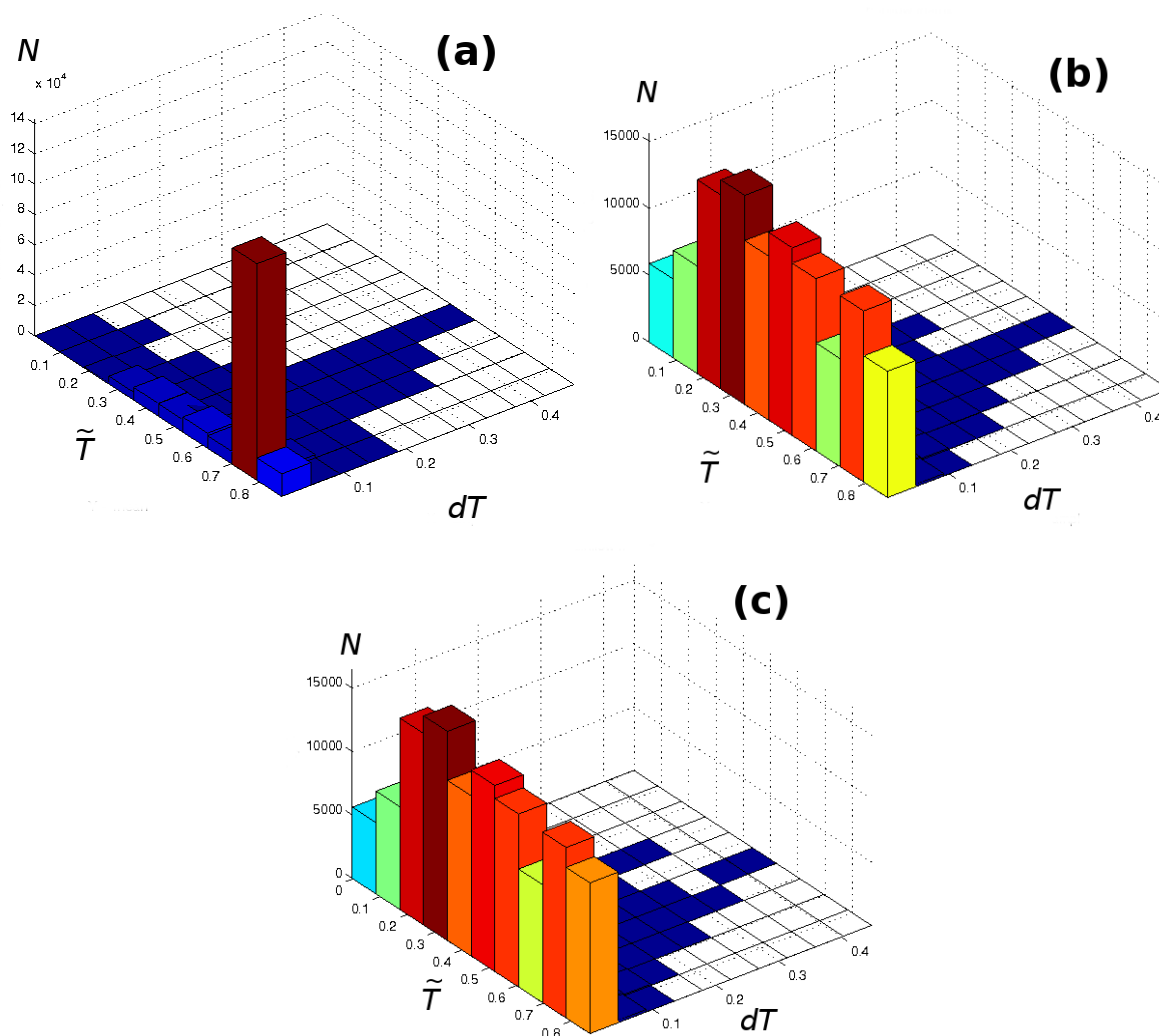
Having a time-series $X(t)$ for $0 < t < T$, let $N(t)$ be the number of counted cycles with maximum M_k and minimum $m_k < M_k$ and let $N_T(u, v)$ be the count distribution yielding the number of cycles counted in $X(t)$ such that $m_k < v \leq u < M_k$. The rainflow counting method assumes that the count intensity $\mu(u, v)$ is the asymptotic behavior of the expected value of the count distribution per time unit:

$$\mu(u, v) = \lim_{T \rightarrow \infty} \frac{E[N_T(u, v)]}{T} \quad (9)$$

In the context of fatigue analysis, the so-called Markov matrix¹ retrieves the number of load cycles of a given amplitude ΔT as a function of the mean value of the observed load during each load cycle \tilde{T} . In Fig. 7a and 7b we plot the Markov matrix of the observed load in AV4 and AV5 respectively. In both

¹ The term “Markov matrix” is used here for the plots shown in Fig. 7 and is standard in the context of engineering for fatigue analysis. It should not be confused with the terms “Markov process” and “Markov condition” used in previous sections, standard in the field of Statistical Physics, with which other different matrix - e.g. transition matrices - may be associated.

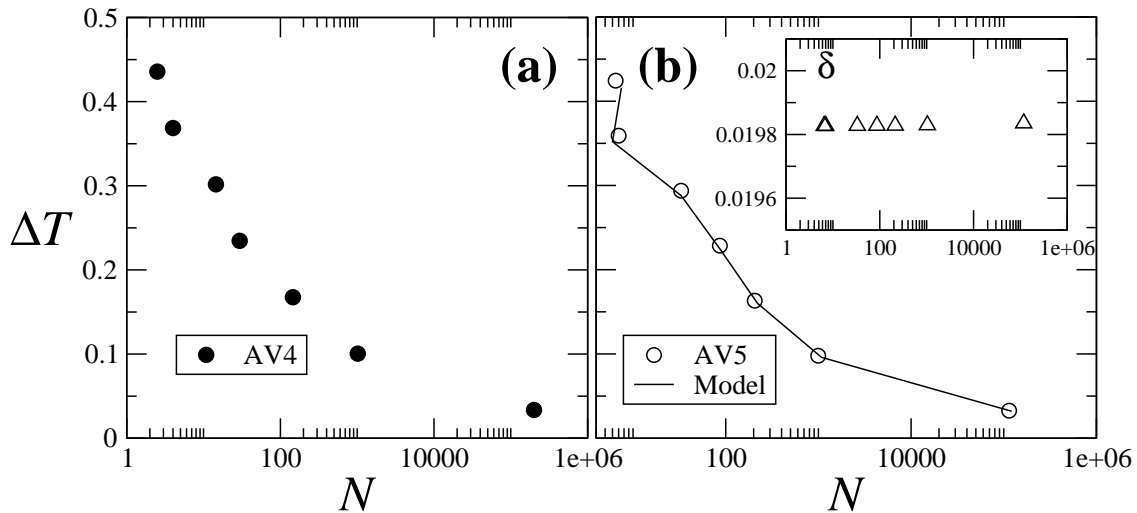
Figure 7. Plot of the Markov matrices, i.e. histograms of the number of cycles N as a function of the mean value of every load cycle, \tilde{T} , and the cycle amplitude itself ΔT for (a) the torque measurements of AV4, (b) the torque measurements of AV5, and (c) the torque estimates of AV5.



cases most of the cycles have an amplitude smaller than 0.5, in units of the maximum value of the load. While at AV4 such amplitudes are observed for large loads, around 0.7, at AV5 such amplitudes are also observed in the remaining range of values, being predominant in the lower load region, around 0.3. The reconstructed load series for AV5, shown in Fig. 7c, however retrieves a good estimate of the full range of values, still with same deviation for the highest load values.

The difference between the observed Markov matrices for AV4 and AV5, with AV5 showing a broader range of torque strengths can be explained by considering the location of each turbine with respect to the main wind directions. As sketched in Fig. 2, AV4 lies westerly from AV5, which lies in the middle of four neighboring wind turbines. Further, the main wind directions are southwest and east-northeast. Thus, the wake effects on AV5 should be stronger than on AV4 and consequently the optimal operation is not as frequent.

Figure 8. Rainflow counting (RFC) of the load (torque) series at (a) AV4 (the data set used for deriving the drift and diffusion of the torque model plotted in Fig. 5) and (b) AV5. While the measurements at AV4 were used for deriving the Langevin model, for AV5 one uses the derived model for reconstructing the data and compare the estimated loads with the observed ones. In the inset we show the relative deviation η from Eq. (10) of the estimate with respect to the experimental results.



Similarly to what we did with Markov matrices we compute the rainflow counting (RFC) for AV4 (bullets in Fig. 8a) and AV5 (circles in Fig. 8b). While the RFC spectra of AV4 and AV5 are qualitatively different, the Langevin model applied to AV5 retrieves a correct estimation of the rainflow spectra. In the inset of Fig. 8b one sees the relative error

$$\eta = \frac{A_r - A_e}{A_r}, \quad (10)$$

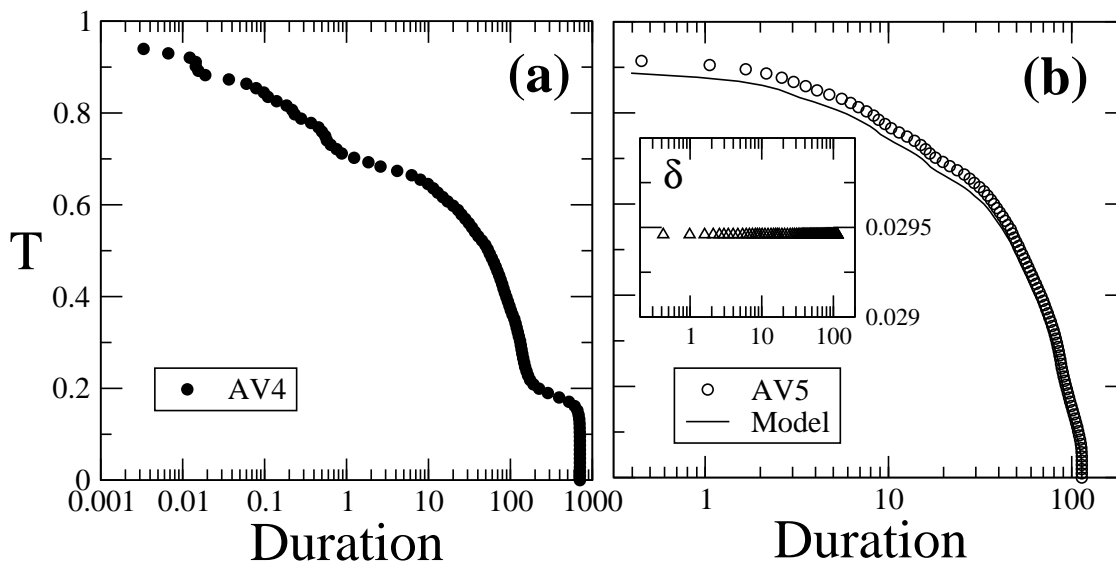
where A_r and A_e are the amplitudes observed for the real and estimated values. The relative errors of the rainflow counting for the estimates is less than 2 %.

Finally, the load duration distribution (LDD) shows the amount of time a load with a given amplitude is observed, retrieving the energy consumed by the system which is no more than the integral of the load duration distribution. As shown in Fig. 9, similarly to what is observed for the RFC, the LDD is also properly reproduced for sufficiently sampled loads (largest values).

The analysis presented in this work does not take into account the wake effects, which are very important for fatigue loads in wind turbines placed in large off-shore farms. As one sees in Fig. 2, from the main wind directions during January 2013 turbine AV5 lies within the wake of AV4. Still, our method was able to accurately predict the fatigue load observed in AV5. This can be explained by noticing that the evolution of the torque in AV5 is conditioned to the wind velocity measurements taken at its nacelle anemometer, which is able to capture the observed turbulence intensity, even under the wake effect from turbine AV4.

4. Conclusions

Figure 9. Load duration distribution (LDD) observed at the load series at (a) AV4 and (b) AV5. While for AV4 the empirical data was used for deriving the model, for AV5 one uses the derived model for reconstructing the data and compare the estimated loads with the observed ones. In the inset we show the relative deviation η shown in Eq. (10) of the estimate with respect to the results for the measurements.



In this paper we applied a framework to one single turbine of Alpha Ventus wind farm for reproducing the loads observed in other similar wind turbines of the same wind farm. The framework consists of the derivation of a stochastic evolution equation for the loads constrained to the wind speed observed at each wind turbine. Using rainflow counting methods and load duration distributions to empirical and modeled data we show that our framework is able to accurately estimate fatigue loads. In a more general context, this procedure can be applied to other properties one wants to access for monitoring and controlling wind turbines.

We stress that the coefficients used to reconstruct the torque at the second turbine are obtained only from the torque and wind velocity at the first turbine. The torque reconstruction is then performed by taken the wind velocity at the second turbine as input parameter. Notice that the coefficients are taken directly from the numerical derivation (Figs. 5) in only one realization. This is possible due to the coupling between v and T which is assumed to be the same for both turbines.

Two points should be stressed for future work. First, the conditional Langevin model here presented and applied has some limitations. Since it is based on the integration of a stochastic differential equation of the load, using empirical input – the wind velocity – in time periods during which no measurements are available, additional assumptions would have to be taken for reconstructing the torque during that period. Moreover, our analysis assumes that the wind velocity field to which the turbine reacts can be completely described by the single anemometer measurements; though such assumption can be taken as a first approximation to the wind velocity field, some properly defined rotor-effective velocity may improve the reconstruction in our model.

Second, having shown the ability of our method to predict one particular load type, namely the one on the drive train, a systematic study of how it works for the rest of the loads on a wind turbine shall proceed. These points will be addressed in a future work.

Acknowledgments

The authors thank Philip Rinn and David Bastine for useful discussions. This work is funded by the German Environment Ministry as part of the research project “Probabilistic loads description, monitoring, and reduction for the next generation offshore wind turbines (OWEA Loads)” under grant number 0325577B. The authors also thank Senvion SE for providing the data here analyzed.

Author Contributions

PGL and IH performed the simulations. PGL and MW prepared the manuscript. JP proposed the ideas and methodologies here proposed. All authors revised the text and output results.

Conflicts of Interest

The authors declare no conflict of interest.

References

1. Johnson, G. *Wind Energy Systems*; Kansas State University, 2006.
2. T. Mücke, D.K.; Peinke, J. Atmospheric turbulence and its influence on the alternating loads on wind turbines. *Wind Energy* **2011**, *14*, 301–316.
3. P. Milan, M.W.; Peinke, J. Turbulent Character of Wind Energy. *Phys. Rev. Lett.* **2013**, *110*, 138701.
4. Burton, T.; Sharpe, D.; Jenkins, N.; Bossanyi, E. *Wind Energy Handbook*; Wiley, 2001.
5. Moriarty, P. Database for validation of design load extrapolation techniques. *Wind Energy* **2008**, *11*, 559–576.
6. Freudenreich, K.; Argyriadis, K. Wind turbine load level based on extrapolation and simplified methods. *Wind Energy* **2008**, *11*, 589–600.
7. Ragan, P.; Manuel, L. Comparing Estimates of Wind Turbine Fatigue Loads using Time-Domain and spectral Methods. *Wind Engineering* **2007**, *31*, 83–99.
8. Rinn, P.; Wächter, M.; Peinke, J. *Private communication* **2013**.
9. Lind, P.; Wächter, M.; Peinke, J. Reconstructing the intermittent dynamics of the torque in wind turbines. *Journal of Physics: Conf. Ser.* **2014**, *524*, 012179.
10. Milan, P.; Mücke, T.; Kleinhans, D.; Peinke, J. Langevin power curves from numerical modelling and monitoring of wind energy converters. *Wind Energy* **2013**, p. in print.
11. Friedrich, R.; Peinke, J. Description of a Turbulent Cascade by a Fokker-Planck Equation. *Phys. Rev. Lett.* **1997**, *78*, 863.
12. Friedrich, R.; Peinke, J.; Sahimi, M.; Tabar, M. Approaching complexity by stochastic methods: From biological systems to turbulence. *Phys. Rep.* **2011**, *506*, 87.
13. E. Anahua, S. Barth, J.P. Markovian Power Curves for Wind Turbines. *Wind Energy* **2008**, *11*, 219.
14. Raischel, F.; Scholz, T.; Lopes, V.; Lind, P. Uncovering wind turbine properties through two-dimensional stochastic modeling of wind dynamics. *Physical Review E* **2013**, *88*, 042146.

15. Milan, P.; Wächter, M.; Peinke, J. Stochastic modeling and performance monitoring of wind farm power production. *Journal of Renewable and Sustainable Energy* **2014**, *6*.
16. F.Boettcher.; J.Peinke.; D.Kleinhans.; R.Friedrich.; P.G.Lind.; M.Haase. Reconstruction of complex dynamical systems affected by strong measurement noise. *Physical Review Letters* **2006**, *97*, 090603.
17. P.G.Lind.; M.Haase.; F.Boettcher.; J.Peinke.; D.Kleinhans.; Friedrich, R. Extracting strong measurement noise from stochastic time series: applications to empirical data. *Physical Review E* **2010**, *81*, 041125.
18. Risken, H. *The Fokker-Planck Equation*; Springer: Heidelberg, 1984.
19. Gottschall, J.; Peinke, J. *New Journal of Physics* **2008**, *10*, 083034.
20. Milan, P.; Wächter, M.; Peinke, J. Wind energy: a turbulent, intermittent resource. *Private communication* **2013**.
21. Matsuishi, M.; Endo, T. Fatigue of metals subjected to varying stress. *Japan Soc. Mech. Engineering* **1968**.
22. Rychlik, I. **A new definition of the rainflow cycle counting method.** *Int. J. Fatigue* **1987**, *9*, 119–121.

© 2014 by the authors; licensee MDPI, Basel, Switzerland. This article is an open access article distributed under the terms and conditions of the Creative Commons Attribution license (<http://creativecommons.org/licenses/by/3.0/>).